

A comprehensive model for the diffusion and hybridization processes of nucleic acid probes in fluorescence in situ hybridization

Joana Lima¹, Paulo Maia¹, Beatriz Magalhães¹, Laura Cerqueira¹, and Nuno Azevedo¹

¹LEPABE

May 5, 2020

Abstract

Fluorescent in situ hybridization (FISH) has been extensively used in the past decades for the detection and localization of nucleic acid sequences or of the microorganisms themselves within samples. However, a mechanistic approach of the whole FISH process is still missing, and the main limiting steps for the hybridization to occur remain unclear. In here, FISH is approached as a particular case of a diffusion-reaction kinetics, where molecular probes move from the hybridization solution to the target RNA site within the cells. Based on literature models, the characteristic times taken by different molecular probes to diffuse across multiple cellular barriers, and the reaction time associated with the formation of the duplex molecular probe-RNA were estimated. Structural and size differences at the membrane level of bacterial and animal cells were considered. For bacterial cells, the limiting step for diffusion is likely to be the peptidoglycan layer (characteristic time of 2700-4524 s), whereas for animal cells the limiting step should be the diffusion of the probe through the bulk (1.8-5.0 s) followed by the diffusion through the lipid membrane (1 s). The information provided here may serve as a basis to optimize FISH protocols.

Introduction

Fluorescent *in situ* hybridization (FISH) is a technique developed in the early '80s that allows the detection and localization of specific DNA or RNA sequences within prokaryotic and eukaryotic cells and tissues^{1,2}. The basic principle of the method relies on the complementarity between a fluorescently-labelled molecular probe (MP), generally composed of DNA, and a specific nucleic acid sequence that is present inside the cell³. A standard FISH procedure includes five steps: fixation, permeabilization, hybridization, washing, and visualization or quantification of the fluorescent signal of the sample. The fixation/permeabilization of the cells is normally performed together, in order to facilitate the uptake of the MPs by destabilizing the cell membrane or envelope without lysis or extensive degradation. Hybridization takes place when a specific MP is fully complementary (or nearly fully complementary) to the target sequence. After washing the non-hybridized or loosely bound MPs, the hybridized MPs can be detected by fluorescence microscopy or quantified by flow-cytometry. FISH may be used both *in vitro* and *in vivo*. In the latter case the hybridization solutions are applied directly into the system, without a prior fixation or permeabilization step⁴.

The hybridization step is critical in FISH, as the efficiency of the hybridization is influenced by different factors that need to be taken into account for optimization. A low-fluorescence hybridization signal can result from cell-dependent limitations, such as low ribosomal content, inaccessibility of the target site, ribonucleases activity or difficulties in the permeabilization of the cellular envelope or membrane⁵. Optimization of the probe design by using nucleic acid mimics such as Peptide Nucleic Acid (PNA) or Locked Nucleic Acid (LNA) can overcome most of these limitations, improving probe specificity and sensitivity⁶. Also, in the case of FISH in fixed cells or tissues, the cellular permeabilization can be further enhanced by using

different chemical fixatives to create pores in the cell membrane/envelope. Other parameters, such as the hybridization temperature and composition of the hybridization solution also compromise the success of the hybridization^{6,7}.

Despite the extended use of FISH for several decades in different fields, a mechanistic approach of the process as a whole is still missing. In their seminal work, Yilmaz *et al.*⁸ were able to develop a model which predicts the hybridization efficiency in FISH based on the affinity of the probe to the target rRNA. Although their approach quite accurately predicts the hybridization efficiency compared to standard prediction methods using the mid-transition temperature (T_m), it only takes into consideration the accessibility of the MPs to the rRNA as the limiting step in FISH, excluding diffusional barriers during the process.

In here, we approach FISH as a particular case of a diffusion-reaction kinetics, similar to other engineering problems that involve diffusion and mass transfer of chemical species within physical and biological systems and a subsequent chemical reaction. Based on literature models, we estimated the characteristic times taken by different DNA-MPs to cross several diffusional barriers and reach the molecular target. As different cell-types impose distinctive barriers for diffusion, in this approach both bacterial, including gram-negative and gram-positive bacteria, and animal cells are considered. The final goal is to assess which of the diffusional or reaction steps take longer and, hence, have a higher time contribution to the 30-90 minutes characteristic of a FISH procedure.

The journey: from the bulk solution to the target RNA site

As stated above, the transport of chemical species within physical systems is ubiquitous on different engineering disciplines, such as chemical and biological engineering. Taking as an example the oxygen transport in bioreactors, it is possible to make an analogy with the transport of the MP from the bulk solution to the reaction site within the cells (Fig. 1).

In bioreactors, the oxygen is transferred from the gas bubbles through different interfaces, until it reaches the cells for uptake (Fig. 1A)^{9,10}. This way, the first interfaces involve the transfer of oxygen from the gas bubbles to the liquid phase (gas-liquid interface), and the diffusion of oxygen through the bulk liquid (liquid-cell interface). The subsequent interfaces involve the cellular uptake of oxygen from the bulk to and within the cytoplasm to the reaction site. In this model, the variation of the dissolved oxygen's concentration in time within the bioreactor depends on the oxygen transfer rate (OTR) and on the oxygen uptake rate (OUR).

Analogously to oxygen transfer, for the MP to reach its target, it first has to diffuse from the bulk solution, and cross the cellular membrane/envelope and the cytoplasm until it reaches the RNA site for hybridization. The diffusion process is based on a concentration gradient over time (Fig. 1B). It is important to notice that, in contrast to oxygen in aerobic bioreactors, the MPs are not continuously added to the system. Instead, the quantity of the MP applied is significantly higher than the number of cells/RNA available for the reaction, in order to ensure a high concentration gradient throughout the entire process. In fact, in a standard *in vitro* FISH procedure there are around 200 MPs per ribosome. It is important to notice that the steps regarding oxygen transfer from the interior of the bubble to the gas-liquid interface and then to the bulk (Fig. 1A, step 1-3) are not applicable in a probe diffusion scenario, as the MPs are already in suspension.

Additionally, in the oxygen transport models, a liquid film around the cells/solid particle is considered (Fig. 1A step 5 and Fig. 1B step 2). The film theory is the simplest premise for interfacial mass transfer, and assumes the existence of a stagnant film, also called unstirred layer, near every interface. It represents the resistance to mass transfer that might occur near an interface, and is almost always hypothetical since the motion of the fluid occurs even in a solid interface¹². Due to the lack of available data for the MP's concentrations in the interface, an overall process, where the cellular membrane/envelope is the first barrier for the MP's diffusion from the bulk solution to the cytoplasm of the cells, can be considered instead (Fig. 1B, step 2).

The characteristic time is defined as an estimation of the order of magnitude of the time required for a process to reach equilibrium. In chemical engineering, it describes the dynamics of a system, for instance the residence time in well-stirred tanks¹³. In here, the characteristic time will give an estimation of the limiting step for diffusion and provide further insights on the circumstances under which FISH needs to be approached as a diffusional problem or a reaction kinetics problem.

In the following sections, the characteristic times associated with the transport through the bulk liquid, the diffusion across the cell membrane/envelope and in the cytoplasm, and, finally, the reaction of the MPs with their target RNA will be estimated for 10 and 40 base pairs (bp) DNA-MPs. The diffusion of the MPs through the cell membrane/envelope is further characterized taking into account the cellular differences between *E. coli*, *Bacillus subtilis* (*B. subtilis*) and HeLa cells, as respective models of gram-negative bacteria, gram-positive bacteria and animal cells.

Diffusion of the MPs in the bulk liquid

To calculate the characteristic time in the bulk solution, i.e. the time necessary for a MP to reach a cellular interface, the diffusion coefficient in the bulk (D_0) first has to be determined. Subsequently the characteristic time of this phase must be calculated, by applying the mean-square displacement of a molecule in the medium (MSD).

The diffusion coefficient can simply be determined by considering the DNA mobility in water¹⁴ according to Eq. 1:

$$D_0 = 4.9 \times 10^{-6} [\text{bp size}]^{-0.72} \text{ (Eq. 1)}$$

where D_0 represents the diffusion and bp size represents the number of nucleotides present in the DNA. This equation is valid for DNA strands ranging from 21 to 6000 bp but was developed for double stranded DNA in water. Despite the lack of studies regarding the relationship between single stranded DNA and its size, it has been demonstrated that a rhodamine-labelled 30 bp single-stranded DNA has a diffusion coefficient of $6.2 \times 10^{-11} \text{ m}^2/\text{s}$ in a water solution¹⁵. This value is in the same order of magnitude as a of 9.34×10^{-11} and $3.44 \times 10^{-11} \text{ m}^2/\text{s}$ calculated with Eq. 1, for a 10 bp and 40 bp MP, respectively.

It is also important to bear in mind that the hybridization solution is more viscous than water, due to the presence of dextran sulphate¹⁶, which may affect diffusion by decreasing the motion of the MP. As such, the diffusion coefficients for 10bp and 40 bp DNA-MPs were also calculated using the viscosity values of two 10% (wt/vol) dextran-hybridization solutions: one containing a low molecular weight dextran of 10 kDa (with a viscosity of 2 mPa.s at 30 °C)¹⁷ and another containing 500 kDa dextran (with a viscosity of 57.2 mPa.s, at 25 °C)¹⁶ (supplementary material). The dextran of 500 kDa is used in particular cases to enhance the probe hybridization rate by artificially increasing the MP's concentration due to the reduction of the available physical space^{16,18,19}. Since Eq. 1 does not take into consideration physicochemical parameters such as the viscosity, the diffusion coefficient for a 500 kDa hybridization solution was calculated using the Stokes-Einstein (SE) equation adapted for non-spherical DNA-MP molecules (Supplementary material). This value was used to calculate the characteristic time of the MP's diffusion in a highly viscous hybridization solution and to modulate the MP's diffusion in an extreme scenario. In the case of the hybridization solution containing dextran sulphate of 10 kDa, Eq. 1 provides similar values compared to the SE equation. The molecular weight of the dextran used in the hybridization solution can be a limiting factor for diffusion in FISH. Particularly for gram-positive bacteria, low-viscosity solutions have shown to provide better results in terms of fluorescent signal¹⁶.

To determine the MSD and calculate the characteristic time, the following three-dimensional equation was applied:

$$\langle r(n)^2 \rangle = 6D_0t \text{ (Eq. 2)}$$

Where r is the average displacement of a molecule over time, D_0 is the diffusion coefficient, as calculated above, and t is the time interval of the simulation²⁰. For simplicity, Eq. 1 was used to calculate the characteristic time of diffusion of the MPs in a hybridization solution containing 10kDa dextran.

To calculate the MSD, it was assumed that the MPs and the cells are homogeneously distributed in the bulk solution. That way, the total volume of the bulk was divided by the number of cells present in the solution, assuming that each cell occupies a defined geometric volume (Fig. 2).

In the case of non-spherical cells, the distance between each cell, equally distributed in the medium, is dependent on its size and orientation. As such, in here, the different layers of the cells were individually characterized, using representative organisms – *E. coli* for gram-negative bacteria, *B. subtilis* for gram-positive bacteria and HeLa for animal cells. Rod-shaped cells can be considered as spherocylinders with radius r and total length L , while spherical cells are modelled as spheres with radius r (as further demonstrated in Table 1). Bacterial cells often present a rod-shape and, in here, HeLa cells were considered spherical. Since the cell-size of the models selected for gram-positive and –negative bacteria is similar, an average L and r were used instead (Table 1).

In the bulk solution, the size of the different cells influences the diffusional time. Animal cells are approximately 20 times larger than bacterial cells, and thus the probability of a MP to encounter a cell in the same bulk volume is higher, resulting in a faster characteristic time. In addition, it is important to notice that this means that for less concentrated samples the characteristic time associated with the diffusion in the bulk medium will also increase (Fig. 3).

By combining the diffusion coefficients calculated using Eq. 1 with Eq. 2, the characteristic diffusion times of MPs of different sizes and in different cells were determined. In the bulk solution, a 10 bp MP takes around 5.55 s to encounter a bacterial cell and 1.84 s to encounter an animal cell, while a 40 bp MP takes 15 s and 5 s, respectively. Moreover, the diffusion coefficients calculated for the 10 and 40 bp MPs in the bulk solution (using Eq. 1) were respectively $9.3 \times 10^{-11} \text{ m}^2/\text{s}$ and $3.4 \times 10^{-11} \text{ m}^2/\text{s}$, which are similar to the ones determined by Robertson *et al.*²¹ for similar-length linear DNA molecules in buffer solutions (specifically, $9.7 \times 10^{-11} \text{ m}^2/\text{s}$ for an 11 bp-DNA molecule and $4.37 \times 10^{-11} \text{ m}^2/\text{s}$ for a 45 bp-DNA molecule).

Diffusion of the MPs through the cell membrane/envelope

In this section, the diffusional path of the MPs through the cell membrane/envelope of the bacterial and mammalian cells, as they move from the bulk to the cytoplasm, is explored. In addition to differing in shape and size, the boundaries of the cells are constituted by structures with different layers and composition (Fig. 4). For instance, animal cells only possess a phospholipidic barrier, the cytoplasmic membrane. Bacterial cells possess an added barrier, the cell envelope, which by its turn has several layers, which differ between gram-positive and gram-negative microorganisms. The gram-negative bacterial cell envelope is constituted by an outer membrane, followed by the periplasmic space which comprises a thin peptidoglycan layer, and the inner cytoplasmic membrane, a phospholipid bilayer (Fig. 4). The periplasmic space normally presents a higher viscosity compared to the cytoplasm due to the presence of small molecules and it is often considered a “crowded” space²². The gram-positive bacterial cell envelope does not have an outer membrane and the peptidoglycan layer is thicker than the one present in gram-negative bacteria, followed by the cytoplasmic membrane (Fig. 4).

Moreover, both bacterial and mammalian cells have proteins channels and other components in their membranes that are responsible for the transport of molecules (Fig. 4). It is a complex structural and functional system, and a comprehensive review about this subject can be found in Santos *et al.*²³. The structural and chemical differences at the membrane level affect the diffusion of the MPs in the different organisms. Table 1 summarizes the average dimensions of each barrier for the different cell models here defined. For bacterial cells the capsule was not considered and the dimensions displayed for the other barriers are purely reference values, since r and L depend on the growth phase, temperature and available nutrients, among

other variables²⁴. The thickness of each layer was set based on the average of available experimental values. In theory, a lipid bilayer has a thickness of around 4 nm²⁵. However, and most likely due to the extra constituents of the outer membrane, such as proteins and lipopolysaccharides (LPS)²⁶, the outer membrane of gram-negative cells is sometimes considered to be thicker than the cytoplasmic membrane. In here, the core size of the bilayer was considered, keeping in mind that the diffusion in this layer may be slower than in the inner membrane.

To facilitate the interpretation, the different layers were grouped in terms of composition. The first barrier discussed here is the lipidic membrane or cytoplasmic membrane, which is the first barrier that the MPs encounter in animal cells. The outer membrane of gram-negative bacteria is also included in the lipid membranes section. The next barriers discussed are the periplasm of gram-negative bacteria followed by the peptidoglycan layers of both gram-positive and gram-negative bacteria. The latter is the first physical barrier for the MP in gram-positive bacteria, and is similar in terms of structure and chemical composition in both grams, varying mainly in thickness²⁶.

Molecular diffusion in lipid membranes

As mentioned above, and in spite of composition differences that might affect the MP's diffusion, the cytoplasmic membrane of gram-positive bacteria, both membranes (outer and inner membrane) of gram-negative bacteria, and the cytoplasmic membrane of animal cells are approached in the same manner.

Considering the importance of nucleic acids diffusion in lipid membranes, there is a remarkable lack of studies for modelling this process, both in bacterial and animal cells. In one of the few existing studies regarding this issue, the diffusion time of DNA probes in lipid membranes has been estimated by tracking the formation of endosomes after injecting DNA into the outer side of a liposome. For an oligonucleotide of 21 bp, the process takes around 1 s³⁵. For *in vivo* hybridization, this value should be considered the lowest possible diffusion time, because it is well known that proteins and other molecules can obstruct and bind to MPs, decreasing the diffusion coefficient³⁶. Although no exact equation is available to model this process for the probe of 10 and 40 bp, this information can be used as an indication of the characteristic time a MP takes to go through a lipid membrane.

Molecular diffusion in the periplasm of gram-negative bacteria

In gram-negative bacteria, the periplasm is located between the outer and the cytoplasmic membranes and is about 13-25 nm thick³⁷. In addition to the peptidoglycan layer, the periplasmic space contains a high concentration of other small molecules like amino acids and peptides that contribute to the increase of viscosity in this interface³⁸. As a result, the periplasm seems to be a gel-like matrix, which makes each molecule experience an effective viscosity during movement and, as such, the molecular diffusion in this "crowded" system diverges from a normal Brownian motion (as described in the bulk). There is limited information on particle diffusion through the periplasm, especially for nucleic acids. Most studies report lateral diffusion of proteins in different membrane layers. Such is the case of the work of Mullineaux *et al.*³⁹, which explores the lateral diffusion of the globular Green Fluorescence Protein (GFP) in the cytoplasm, periplasm, and plasma membrane of *E. coli*. They established that the diffusion in the periplasm (D_{peri}) is about three times smaller than in the cytoplasm (D_{cyto}), but highlighted that, in terms of physical properties, the periplasm is a relatively fluid environment, in comparison to the cytoplasm. For these reasons, it was assumed that is in the same order of magnitude as . values are provided in the section concerning the diffusion of the MP in the cytoplasm. Using the values and Eq. 1, a 10 bp probe takes 3.8×10^{-7} s to diffuse through the periplasm, while a 40 bp probe, with a larger radius, takes 1.8×10^{-6} s.

Molecular diffusion in the peptidoglycan

The peptidoglycan layer is structurally similar in gram-negative and -positive bacteria, mostly varying in thickness. In FISH, the diffusion of MPs through the peptidoglycan layer most likely represents the limiting step in both Grams. This is true even for gram-negative bacteria despite of their severally restrictive outer membrane, because of the fixation steps prior to the addition of the MPs, which create pores in the outer membrane, allowing the MPs to directly cross from the extracellular space to the peptidoglycan layer. Gram-negative bacteria have a thin peptidoglycan layer, whereas the peptidoglycan of gram-positive bacteria can be up to 100 nm thick²⁶. Overcoming this layer is crucial for a successful FISH procedure, especially in gram-positive bacteria, where longer hybridization times are required compared to gram-negative bacteria (normally the FISH procedure takes approximately 120 min for the detection of gram-positive bacteria and 60 min for gram-negative)¹⁶, most likely due to the differences in thickness. The thickness of the peptidoglycan makes it particularly important to proceed with the permeabilization of fixed gram-positive bacteria, or with the enzymatic hydrolysis of the peptidoglycan prior to the hybridization of large MPs, in order to have a detectable fluorescence signal⁴⁰.

Since there is no data in the literature related to the diffusion coefficient of the MPs in the peptidoglycan barrier, the difference between the commonly used experimental hybridization times in FISH for gram-negative and gram-positive bacteria was used to calculate the diffusion coefficient of the MP in the layer for both grams. For gram-positive bacteria, a diffusion coefficient of $3.5 \times 10^{-19} \text{ m}^2/\text{s}$ was obtained, which corresponds to a characteristic diffusion time of 4524 s (75 min). This in agreement with the general concept that the peptidoglycan layer of gram-positive bacteria is one of the most relevant barriers in microbial FISH experiments⁴⁰.

Transport through the cell cytoplasm until the reaction site

Not unlike the periplasm, the cytoplasm is considered a crowded system due to the high concentration of molecules in the medium. In fact, it is estimated that the macromolecular concentration in the cytoplasm is about 400 mg/mL, 30-40 % of its total weight^{41,42}. The presence of these molecules increases the viscosity of the medium, slowing down the diffusion of small molecules ($M_w \sim 170 - 5,500 \text{ KDa}$) by approximately 20-50% when compared to the diffusion in water ($D_{\text{cytoplasm}} < D_{\text{water}}$)⁴³.

Golding and Cox⁴⁴ were the first to introduce the notion that in crowded environments, particles are subjected to a sub-diffusing motion, by examining the motion of fluorescently-labelled mRNA molecules inside *E. coli* cells. They have demonstrated that RNA molecules move discontinuously in such cells, with periods of almost localized motion, separated by fast “jumps” to a new position. This type of diffusion in the cytoplasm is anomalous, due to the molecular crowding, contrasting with the normal Brownian diffusion.

In this situation, the diffusion coefficients can be determined by applying Eq. 3:

$$\ln \left(\frac{D_0}{D_{\text{cyto}}} \right) = \ln \left(\frac{\eta}{\eta_0} \right) = \ln(A) + \left(\frac{\xi^2}{R_h^2} + \frac{\xi^2}{r_p^2} \right)^{\frac{-a}{2}} \quad (\text{Eq. 3})$$

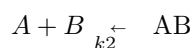
where D_0 is the diffusion coefficient of a macromolecule in water with a viscosity of η_0 , D_{cyto} is the diffusion coefficient of the same macromolecule in the cytoplasm, η is the effective viscosity experienced by the macromolecule when crossing the cytoplasm, r_p is the hydrodynamic radius of the MP, and ξ , R_h , A , and a , are fitting parameters. ξ is an average distance between the surfaces of proteins, R_h is an average hydrodynamic radius of the biggest crowders, A and a is a constant of the order of 1. D_0 can be calculated using Eq. 1, and the diffusion coefficient in the cytoplasm for any particle of interest can be obtained by applying Eq.3. The fitting parameters for the cytoplasm of *E. coli* cells are as follows: $\xi = 0.51 \pm 0.09 \text{ nm}$, $r_p = 42 \pm 9 \text{ nm}$, $\ln(A) = 0$, and $a = 0.53 \pm 0.04$ ⁴⁵. Regarding animal cells, the fitting parameters obtained for HeLa cells are $\xi = 5 \pm 4 \text{ nm}$, $R_h = 86 \text{ nm}$, $A = 0.9 \text{ mPa}\cdot\text{s}$ and $a = 0.49 \pm 0.22$ ⁴⁶.

By applying Eq. 3 it is possible to determine the for 10 bp and 40 bp MPs, which are respectively equal to 7.3×10^{-11} and 1.6×10^{-11} in bacteria, and 1.5×10^{-10} and 5.6×10^{-11} m^2/s in animal cells. Using these values, and applying the MSD equation, the correspondent characteristic times for diffusion of the MPs in the cytoplasm are 2.14×10^{-3} and 1.01×10^{-2} s for bacteria, and 2.79×10^{-2} and 7.65×10^{-2} s for animal cells.

These values were obtained assuming that the RNA is located in the center of the cells, and, as such, the maximum distance taken by the MPs is the radius in the case of HeLa cells or half of the total length of the cell in the case of the *E. coli* and *B. subtilis* cells (Table 1). As it can be observed, the D_{cyto} is higher in animal cells than in bacteria, which is in agreement with the evidence that bacteria have a more crowded cytoplasm than animal cells do⁴⁷.

Reaction of MP with RNA molecules available at the reaction site

The reaction between a nucleic acid sequence and their target RNA site is limited either by the diffusion to the site or the chemical reaction of both molecules. When the reaction is the limiting step, the time taken for it to occur is longer than the diffusional time ($t_{\text{reaction}} \gg t_{\text{diffusion}}$). When the opposite happens, the diffusion is the limiting step, which means that the 2 molecules immediately react at their first encounter. The pathway that the MPs undergo in this step is basically translated in the velocity of the two processes. The DNA-MP hybridization reaction kinetics, where a single-stranded DNA MP species (A) binds to a target RNA (B) to form a duplex (AB), can be expressed as⁴⁸:



And the reaction rate of AB formation is given by

$$\frac{d[AB]}{dt} = k_1 [A] [B] - k_2 [AB] \text{ (Eq. 4)}$$

where [A], and [B] are the concentrations of the reactants A and B, [AB] is the concentration of the product AB, k_1 is the association reaction constant of second order kinetics ($\text{M}^{-1}\text{s}^{-1}$), and k_2 is the dissociation reaction constant of first order (s^{-1}). The total concentration of the two reactants is given by:

$$A_0 = [A] + [AB] \text{ (Eq. 5)}$$

and

$$B_0 = [B] + [AB] \text{ (Eq. 6)}$$

Many hybridization reactions are carried out with excess of MPs to maximize the fluorescence signal and the reaction speed. As demonstrated before, the MPs are in excess compared to the available RNA molecules for hybridization, such that $A_0 \gg B_0$ and reaction kinetics becomes a pseudo first order. The reaction rate equation for pseudo-first order kinetics can be expressed as

$$\frac{d[AB]}{dt} = k_1 A_0 (B_0 - [AB]) - k_2 [AB] \text{ (Eq. 7)}$$

At the initial conditions, $[AB] = 0$ and integrating the above first order equation it is possible to obtain:

$$[AB] = B_0 \frac{A_0}{K + A_0} (1 - e^{-(K + A_0)k_1 t}) \text{ (Eq. 8)}$$

where K denotes the equilibrium dissociation constant defined as k_2/k_1 ⁴⁸. The characteristic time scale of the reaction was calculated using Eq. 8, knowing the association and dissociation constant values available in the literature and assuming a complete hybridization, i.e. all the available RNA molecules are hybridized with the MPs. In this setting, $[B] = 0$, and $[AB] = [B_0]$. At $t=0$, $[A] = 2.0 \times 10^{-7}$ M and $[B] = 1.03 \times 10^{-6}$ M (4×10^6 ribosomes) was considered for HeLa cells, whereas $[B] = 3.54 \times 10^{-5}$ M (3×10^4 ribosomes) was considered for *E. coli* cells⁴⁹. For simplification, it was assumed that there was a homogeneous distribution of probes and RNA in all cells.

Regarding the kinetic parameters, no values are available for the specific MP sizes chosen for this study, to the best of the authors' knowledge. Instead, a $k_1 = 2.9 \times 10^6 \text{M}^{-1}\text{s}^{-1}$ and a $k_2 = 0.3 \text{s}^{-1}$ for a 16 bp DNA probe⁵¹ was used, which are values for HeLa cells. Using these values and Eq. 8, it was possible to obtain the characteristic time of the reaction, which is approximately of 0.02 s for HeLa cells, and 9.8×10^{-4} s for *E. coli* cells.

Discussion

Determining the characteristic time of diffusion of MPs is of great value in biochemical engineering, and, specifically, it could help defining the limiting step in the hybridization process in FISH, establishing the problematic of the hybridization efficiency either as an equilibrium problem or a kinetic problem. In here, the characteristic time spent crossing each barrier in the cell by the MPs in a FISH procedure, from the bulk solution to the reaction site, was determined, taking into account the chemical and physical differences between bacterial and animal cells. The obtained diffusional characteristic times are summarized in Table 2.

Overall, the limiting step for the diffusion in bacterial cells seems to be the peptidoglycan layer. In animal cells, the cytoplasmic membrane does not impose a significant barrier for diffusion and, therefore, the limiting step for the diffusion of MPs is more likely to be in the bulk solution or in the hybridization reaction step.

There are very few studies regarding the diffusion of nucleic acids through bacterial and animal cells, and, for that reason, several adjustments were made to simplify the model here presented. For instance, the gram-negative outer membrane is considered an asymmetric lipid bilayer, whose inner side is composed of phospholipids and whose outer side is a LPS layer. The LPS net negative charge is higher than the negatively charged phospholipids, and it is known to decrease the permeability of the outer membrane to hydrophobic compounds. In *E. coli*, studies show that the outer membrane limits the penetration of PNA, with the LPSs as the major accountable factors⁵². The neutral charge of PNA and its relatively high hydrophobicity compared to charged oligonucleotides was pinpointed as the probable cause for the PNA's limited diffusion in the *E. coli*'s outer membrane. After passing this initial barrier, the molecules face the peptidoglycan layer, which in *E. coli*, due to the thickness of the layer, was shown to not impose a significant barrier to PNA passage⁵². This might not be true for gram-positive bacteria, which, due to the lack of an outer membrane with LPSs as the first protection barrier, instead present teichoic acids that limit the permeability to hydrophobic compounds, and a thicker peptidoglycan layer that may significantly retard the penetration of PNA. In the case of negatively charged nucleic acids, such as DNA and LNA, they need to overcome the electrostatic repulsion of the LPSs, also negatively charged, in order to cross the outer membrane. Moreover, the outer membrane also presents channel-forming proteins, called porins, which allow the passage of hydrophilic compounds and large molecules⁵³. The passage of most nucleic acids with around 2–4 kDa in size across the outer membrane is very unlikely because porins are only permeable to molecules with 0.7–0.8 nm in diameter and 600 Da in molecular weight⁵⁴.

In the peptidoglycan layer, measurements of the penetration of polysaccharides show that the peptidoglycan and its associated anionic polymers provide an open network which is accessible to molecules of molecular weights in the range 30 kDa to 57 kDa. The molecular weight of the MPs used in here is smaller than this range (3 kDa and 12 kDa for 10 bp and 40 bp, respectively), and probably because of the small MP size the diffusion of these molecules is facilitated. The permeability properties of gram-positive cell wall may be dependent upon the nature of the peptidoglycan, particularly its degree of cross-linking and the glycan chain length³⁶. Moreover, the fixation and permeabilization steps, typically performed in FISH/FIVH, may lead to altered membrane structures, facilitating the diffusion through this barrier.

All of these particular specifications at the bacterial cell envelope level were not taken into account in the model, and therefore the characteristic times showed in Table 2 caress from further optimization, since they might be underestimated specially for the diffusion in the outer membrane of gram-negative bacteria, and overestimated in the case of the diffusion in the peptidoglycan layer.

For animal cells, passive diffusion of nucleic acid mimics is very unlikely because the phospholipid bilayer only allows the passage of small, relatively hydrophobic and uncharged molecules, limiting the uptake of charged molecules of any size⁵⁵. However, there are studies indicating that antisense oligonucleotides may be easily and rapidly internalized by endocytosis, and then transported through multiple membrane-bound intracellular compartments, which may retard cytoplasmic diffusion⁵⁶. Therefore, the diffusion of molecular probes might not be limited by the phospholipid membrane of mammalian cells, yet it might be compromised in the cytoplasm and/or bulk solution.

Considering the hybridization reaction of the MPs, the values presented in Table 2 were obtained assuming a two-state model to simplify the system. However, during hybridization the MPs and the target RNA can undergo other configurations (folded or unfolded), as presented in the work of Yilmaz *et al.*⁵⁷. This way, the reaction time might be slower than the one presented here. Moreover, parameters related to probe affinity, such as Gibbs energy, were not considered, and the model was built only considering the kinetics of the hybridization. The fluorescence intensity of the cells and, thus, of the FISH method, is influenced by the accessibility and affinity of the MPs to their target site, which can be defined thermodynamically by an overall Gibbs free energy change ($\Delta G^{\circ}_{\text{overall}}$). Thermodynamic measurements should be further associated with hybridization kinetics studies, in order to obtain a more realistic model of the MPs hybridization in FISH^{57,58}. Also, the diffusional time for a MP to cross the ribosome and reach the target RNA was not considered, which may affect the overall time of a FISH procedure. Ridgway *et al.*⁵⁹, simulated the diffusion and reaction kinetics in a crowded virtual cytoplasm, using *E. coli* as a model. They established that the diffusion time necessary for the largest particles in the cytoplasm to cross a ribosome is roughly around 10^{-7} s and 10^{-6} s.

FRAP takes advantage of the permanent loss of the fluorescent signal when exposed to a beam of intense light (bleaching). After bleaching of the selected region, the photobleached molecules diffuse out of the bleached area and fluorescent molecules diffuse into it, allowing the recovery of fluorescence in the same area. Using a low-intensity light source, it is possible to image and monitor the movement of the molecules, and, as such, obtain the time necessary to recover the fluorescence signal in the selected region, or the recovery-rate constant. Such parameter is related with the diffusion coefficient of the molecules in that setting⁶⁰. FRAP has been used to study the motion of fluorescent molecules in solution, on cell surfaces and within the cytoplasm^{39,61,62}. The model presented here could greatly benefit from well-designed FRAP experiments to determine the diffusion coefficients of the MPs in each diffusional barrier, ultimately leading to an overall diffusion and uptake rate for the MPs in FISH, in order to better fit the approximation to the oxygen transfer model.

Conclusion

The development of a more holistic mechanistic model allows the maximization of the FISH's efficiency helping in the optimization of probe design and probe concentration. It is however apparent from this work that many of the characteristic time values obtained lack strong experimental support. In future works, these parameters could be further assessed experimentally, using fluorescent microscopy techniques such as fluorescence recovery after photobleaching (FRAP). With the current data, it was estimated that for bacterial cells the limiting step for diffusion is likely to be the peptidoglycan layer, whereas for animal cells the limiting step is more likely to be the diffusion of the probe through the bulk medium followed by the diffusion through the lipid membrane. The information provided here may serve as a basis to optimize FISH protocols and as a conceptual background for the interpretation of FISH as a specific case of a diffusion-reaction process.

Acknowledgments

This work was financially supported by: Base Funding - UIDB/00511/2020 of the Laboratory for Process Engineering, Environment, Biotechnology and Energy – LEPABE - funded by national funds through the FCT/MCTES (PIDDAC). Additionally, Joana Filipa Lima was supported by PhD Grant

SFRH/BDE/51909/2012 by Portuguese Foundation for Science and Technology, and Biomode 2, S.A., and Beatriz T. Magalhaes was supported by PhD Grant SFRH/BD/143491/2019 by FCT. Laura Cerqueira is financed through Project POCI-01-0145-FEDER-029961, funded by FEDER funds through COMPETE2020 – Programa Operacional Competitividade e Internacionalizacao (POCI) and by national funds (PIDDAC) through FCT/MCTES.

References

1. Langer-Safer, P. R., Levine, M. & Ward, D. C. Immunological method for mapping genes on *Drosophila* polytene chromosomes. *Proc. Natl. Acad. Sci.* **79** , 4381–4385 (1982).
2. DeLong, E., Wickham, G. & Pace, N. Phylogenetic stains: ribosomal RNA-based probes for the identification of single cells. *Science (80-.)*. **243** , 1360–1363 (1989).
3. Moter, A. & Gobel, U. B. Fluorescence in situ hybridization (FISH) for direct visualization of microorganisms. *J. Microbiol. Methods***41** , 85–112 (2000).
4. Fontenete, S. *et al.* Towards fluorescence in vivo hybridization (FIVH) detection of *H. pylori* in gastric mucosa using advanced LNA probes. *PLoS One* **10** , (2015).
5. Behrens, S., Fuchs, B. M., Mueller, F. & Amann, R. Is the In Situ Accessibility of the 16S rRNA of *Escherichia coli* for Cy3-Labeled Oligonucleotide Probes Predicted by a Three-Dimensional Structure Model of the 30S Ribosomal Subunit? *Appl. Environ. Microbiol.***69** , 4935–4941 (2003).
6. Fontenete, S., Guimaraes, N., Wengel, J. & Azevedo, N. F. Prediction of melting temperatures in fluorescence in situ hybridization (FISH) procedures using thermodynamic models. *Crit. Rev. Biotechnol.***8551** , 1–12 (2015).
7. Simard, C., Lemieux, R. & Cote, S. Urea substitutes toxic formamide as destabilizing agent in nucleic acid hybridizations with RNA probes. *Electrophoresis* **22** , 2679–2683 (2001).
8. Yilmaz, L. S. & Noguera, D. R. Mechanistic approach to the problem of hybridization efficiency in fluorescent in situ hybridization. *Appl. Environ. Microbiol.* **70** , 7126–39 (2004).
9. Garcia-Ochoa, F., Gomez, E., Santos, V. E. & Merchuk, J. C. Oxygen uptake rate in microbial processes: An overview. *Biochemical Engineering Journal* vol. 49 289–307 (2010).
10. Clark, D. S.; Blanch, H. W. *Biochemical Engineering*. (Marcel Dekker, New York., 1997).
11. Bakshi, S., Siryaporn, A., Goulian, M. & Weisshaar, J. C. Superresolution Imaging of Ribosomes and RNA Polymerase in Live *Escherichia coli* Cells. *Mol. Microbiol.* **85** , 21–38 (2012).
12. Cussler, E. L. Diffusion: Mass Transfer in Fluid Systems. *Engineering Second* , 580 (1997).
13. Corriou, J.-P. & Azzaro-Pantel, C. Process Optimization Strategies. in *Green Process Engineering* 27–48 (CRC Press, 2015). doi:doi:10.1201/b18533-4.
14. Lukacs, G. L. *et al.* Size-dependent DNA mobility in cytoplasm and nucleus. *J. Biol. Chem.* **275** , 1625–1629 (2000).
15. Xu, X.-H. & Yeung, E. S. Direct Measurement of Single-Molecule Diffusion and Photodecomposition in Free Solution. *Science (80-.)*. **275** , 1106–1109 (1997).
16. Rocha, R., Santos, R. S., Madureira, P., Almeida, C. & Azevedo, N. F. Optimization of peptide nucleic acid fluorescence in situ hybridization (PNA-FISH) for the detection of bacteria: The effect of pH, dextran sulfate and probe concentration. *J. Biotechnol.***226** , 1–7 (2016).
17. Algotsson, M. *et al.* Sample preservation method and sample preservation substrate. (2017).

18. Hrabovszky, E. & Petersen, S. L. Increased concentrations of radioisotopically-labeled complementary ribonucleic acid probe, dextran sulfate, and dithiothreitol in the hybridization buffer can improve results of in situ hybridization histochemistry. *J. Histochem. Cytochem.* **50** , 1389–400 (2002).
19. Wahl, G. M., Stern, M. & Stark, G. R. Efficient transfer of large DNA fragments from agarose gels to diazobenzoyloxymethyl-paper and rapid hybridization by using dextran sulfate. *Proc. Natl. Acad. Sci. U. S. A.* **76** , 3683–3687 (1979).
20. Gameiro, D. *et al.* Computational resources and strategies to construct single-molecule metabolic models of microbial cells. *Brief. Bioinform.* bbv096 (2015).
21. Robertson, R. M., Laib, S. & Smith, D. E. Diffusion of isolated DNA molecules: Dependence on length and topology. *Proc. Natl. Acad. Sci.* **103** , 7310–7314 (2006).
22. Mogensen, J. E. & Otzen, D. E. Interactions between folding factors and bacterial outer membrane proteins. *Mol. Microbiol.* **57** , 326–346 (2005).
23. Santos, R. S., Figueiredo, C., Azevedo, N. F., Braeckmans, K. & De Smedt, S. C. Nanomaterials and molecular transporters to overcome the bacterial envelope barrier: Towards advanced delivery of antibiotics. *Adv. Drug Deliv. Rev.* (2017) doi:<https://doi.org/10.1016/j.addr.2017.12.010>.
24. Chien, A.-C., Hill, N. S. & Levin, P. A. Cell Size Control in Bacteria. *Curr. Biol.* **22** , R340–R349 (2012).
25. van Meer, G., Voelker, D. R. & Feigenson, G. W. Membrane lipids: where they are and how they behave. *Nat. Rev. Mol. Cell Biol.* **9** , 112–124 (2008).
26. Silhavy, T., Kahne, D. & Walker, S. The bacterial cell envelope. *Cold Spring Harbor perspectives in biology* vol. 2 1–16 (2010).
27. Katz, A. *et al.* Bacteria Size Determination by Elastic Light Scattering. *IEEE J. Sel. Top. QUANTUM Electron.* **9** , 277–287 (2003).
28. Zhao, L. *et al.* Intracellular water-specific MR of microbead-adherent cells: The HeLa cell intracellular water exchange lifetime. *NMR Biomed.* **21** , 159–164 (2008).
29. Grossman, N., Ron, E. A. & Woldringh, C. L. Changes in cell dimensions during amino acid starvation of *Escherichia coli*. *J. Bacteriol.* **152** , 35–41 (1982).
30. Mitra, K., Ubarretxena-Belandia, I., Taguchi, T., Warren, G. & Engelman, D. M. Modulation of the bilayer thickness of exocytic pathway membranes by membrane proteins rather than cholesterol. *Proc. Natl. Acad. Sci.* **101** , 4083–4088 (2004).
31. Bayer, M. E. Zones of membrane adhesion in the cryofixed envelope of *Escherichia coli*. *J. Struct. Biol.* **107** , 268–280 (1991).
32. Graham, L. L., Beveridge, T. J. & Nanninga, N. Periplasmic space and the concept of the periplasm. *Trends Biochem. Sci.* **16** , 328–329 (2017).
33. Beeby, M., Gumbart, J. C., Roux, B. & Jensen, G. J. Architecture and assembly of the Gram-positive cell wall. *Mol. Microbiol.* **88** , 664–672 (2013).
34. Vollmer, W. & Seligman, S. J. Architecture of peptidoglycan: more data and more models. *Trends Microbiol.* **18** , 59–66 (2010).
35. Angelova, M. I. & Tsoneva, I. Interactions of DNA with giant liposomes. *Chem. Phys. Lipids* **101** , 123–137 (1999).
36. Lambert, P. a. Cellular impermeability and uptake of biocides and antibiotics in gram-positive bacteria and mycobacteria. *J Appl Microbiol* **92** , 46S-54S (2002).

37. Seltmann, G. & Holst, O. Periplasmic Space and Rigid Layer BT - The Bacterial Cell Wall. in (eds. Seltmann, G. & Holst, O.) 103–132 (Springer Berlin Heidelberg, 2002). doi:10.1007/978-3-662-04878-8_3.
38. Holst, O., Moran, A. P. & Brennan, P. J. Chapter 1 - Overview of the glycosylated components of the bacterial cell envelope BT - Microbial Glycobiology. in 1–13 (Academic Press, 2010). doi:https://doi.org/10.1016/B978-0-12-374546-0.00001-8.
39. Mullineaux, C. W. & Kirchhoff, H. Using Fluorescence Recovery After Photobleaching to Measure Lipid Diffusion in Membranes BT - Methods in Membrane Lipids. in (ed. Dopico, A. M.) 267–275 (Humana Press, 2007). doi:10.1007/978-1-59745-519-0_18.
40. Bidnenko, E., Mercier, C., Tremblay, J., Tailliez, P. & Kulakauskas, S. Estimation of the state of the bacterial cell wall by fluorescent In situ hybridization. *Appl. Environ. Microbiol.* **64** , 3059–62 (1998).
41. Zimmerman, S. B. & Trach, S. O. Estimation of macromolecule concentrations and excluded volume effects for the cytoplasm of Escherichia coli. *J. Mol. Biol.* **222** , 599–620 (1991).
42. Fulton, A. B. How crowded is the cytoplasm? *Cell* **30** , 345–347 (1982).
43. Mastro, A. M., Babich, M. A., Taylor, W. D. & Keith, A. D. Diffusion of a small molecule in the cytoplasm of mammalian cells. *Proc. Natl. Acad. Sci.* **81** , 3414–3418 (1984).
44. Golding, I. & Cox, E. C. Physical nature of bacterial cytoplasm. *Phys. Rev. Lett.* **96** , (2006).
45. Kalwarczyk, T., Tabaka, M. & Holyst, R. Biologistics-Diffusion coefficients for complete proteome of Escherichia coli. *Bioinformatics* **28** , 2971–2978 (2012).
46. Kalwarczyk, T. *et al.* Comparative analysis of viscosity of complex liquids and cytoplasm of mammalian cells at the nanoscale. *Nano Lett.* **11** , 2157–2163 (2011).
47. van den Berg, J., Boersma, A. J. & Poolman, B. Microorganisms maintain crowding homeostasis. *Nat. Rev. Microbiol.* **15** , 309–318 (2017).
48. Kilsa Jensen, K., Orum, H., Nielsen, P. E. & Norden, B. Kinetics for hybridization of peptide nucleic acids (PNA) with DNA and RNA studied with the BIAcore technique. *Biochemistry* **36** , 5072–5077 (1997).
49. Scientific, T. Macromolecular Components of E. coli and HeLa Cells. <https://www.thermofisher.com/pt/en/home/references/ambion-tech-support/rna-tools-and-calculators/macromolecular-components-of-e.html>.
50. Noller, H. F. RNA structure: reading the ribosome. *Science* **309** , 1508–14 (2005).
51. Schoen, I., Krammer, H. & Braun, D. Hybridization kinetics is different inside cells. *Proc. Natl. Acad. Sci. U. S. A.* **106** , 21649–21654 (2009).
52. Eriksson, M., Nielsen, P. E. & Good, L. Cell permeabilization and uptake of antisense peptide-peptide nucleic acid (PNA) into Escherichia coli. *J. Biol. Chem.* **277** , 7144–7147 (2002).
53. Nikaido, H. Molecular basis of bacterial outer membrane permeability revisited. *Microbiol. Mol. Biol. Rev.* **67** , 593–656 (2003).
54. Cowan, S. W. *et al.* Crystal structures explain functional properties of two E. coli porins. *Nature* **358** , 727–733 (1992).
55. Cooper, G. M., Hausman, R. E. & Hausman, R. E. *The cell: a molecular approach* . vol. 10 (ASM press Washington, DC, 2000).
56. Koller, E. *et al.* Mechanisms of single-stranded phosphorothioate modified antisense oligonucleotide accumulation in hepatocytes. *Nucleic Acids Res.* **39** , 4795–4807 (2011).

57. Yilmaz, L. S. & Noguera, D. R. Mechanistic approach to the problem of hybridization efficiency in fluorescent in situ hybridization. *Appl. Environ. Microbiol.* **70** , 7126–7139 (2004).
58. Walton, S. P., Stephanopoulos, G. N., Yarmush, M. L. & Roth, C. M. Thermodynamic and Kinetic Characterization of Antisense Oligodeoxynucleotide Binding to a Structured mRNA. *Biophys. J.* **82** , 366–377 (2002).
59. Ridgway, D. *et al.* Coarse-Grained Molecular Simulation of Diffusion and Reaction Kinetics in a Crowded Virtual Cytoplasm. *Biophys. J.* **94** , 3748–3759 (2008).
60. De Los Santos, C., Chang, C.-W., Mycek, M.-A. & Cardullo, R. A. FRAP, FLIM, and FRET: Detection and analysis of cellular dynamics on a molecular scale using fluorescence microscopy. *Mol. Reprod. Dev.* **82** , 587–604 (2015).
61. Schlessinger, J., Axelrod, D., Koppel, D. E., Webb, W. W. & Elson, E. L. Lateral transport of a lipid probe and labeled proteins on a cell membrane. *Science (80-)*. **195** , 307 LP – 309 (1977).
62. Carisey, A., Stroud, M., Tsang, R. & Ballestrem, C. Fluorescence Recovery After Photobleaching BT - Cell Migration: Developmental Methods and Protocols. in (eds. Wells, C. M. & Parsons, M.) 387–402 (Humana Press, 2011). doi:10.1007/978-1-61779-207-6_26.

List of Tables

Table 1. Size of the different layers for bacterial and animal cells, using *E. coli* as a model for gram-negative bacteria, *B. subtilis* for gram-positive and HeLa for animal cells.

Parameter	Gram-negative bacteria (nm)	Gram-positive bacteria (nm)	Animal cells (nm)	References
Cell radius [r]	435	435	10100	11,27,28
Total cell length [L]	2220	2220	-	27,29
Inner membrane thickness	3.5	3.5	3.5	30
Outer membrane thickness	3.5	-	-	31
Periplasm thickness	13	-	-	32
Peptidoglycan thickness	6.4	35.4 ± 8.2	-	33,34

Table 2. Summary of the characteristic times given for 10bp and 40 bp MPs in each diffusional barrier.

	Diffusion characteristic time (s)	Diffusion characteristic time (s)	Diffusion characteristic time (s)	Diffusion characteristic time (s)	Diffusion characteristic time (s)	Diffusion characteristic time (s)
	Gram-negative bacteria (<i>E. coli</i>)	Gram-negative bacteria (<i>E. coli</i>)	Gram-positive bacteria (<i>B. subtilis</i>)	Gram-positive bacteria (<i>B. subtilis</i>)	Animal cell (HeLa cells)	Animal cell (HeLa cells)
Diffusional Barriers	10 bp	40 bp	10 bp	40 bp	10 bp	40 bp
Bulk solution	5.6 - 142	15.1 -313	5.5-141	15.0-310	1.8-46.9	5.0-103
Cell membrane/envelope						

	Diffusion characteris- tic time (s)	Diffusion characteris- tic time (s)	Diffusion characteris- tic time (s)	Diffusion characteris- tic time (s)	Diffusion characteris- tic time (s)	Diffusion characteris- tic time (s)
Lipid membranes	1.0 +	1.0	1.0	1.0	1.0	1.0
Periplasm	3.8×10^{-7}	1.8×10^{-6}	-	-	-	-
Peptidoglycan	2700	2700	4524	4524	-	.
Cytoplasm	2.1×10^{-3}	1.01×10^{-2}	2.1×10^{-3}	1.01×10^{-2}	2.8×10^{-2}	7.7×10^{-2}
Reaction	9.8×10^{-4} (for 16 bp)	9.8×10^{-4} (for 16 bp)	9.8×10^{-4} (for 16 bp)	9.8×10^{-4} (for 16 bp)	0.02 (for 16 bp)	0.02 (for 16 bp)
+ value for the inner membrane only	+ value for the inner membrane only	+ value for the inner membrane only	+ value for the inner membrane only	+ value for the inner membrane only	+ value for the inner membrane only	+ value for the inner membrane only

List of Figures

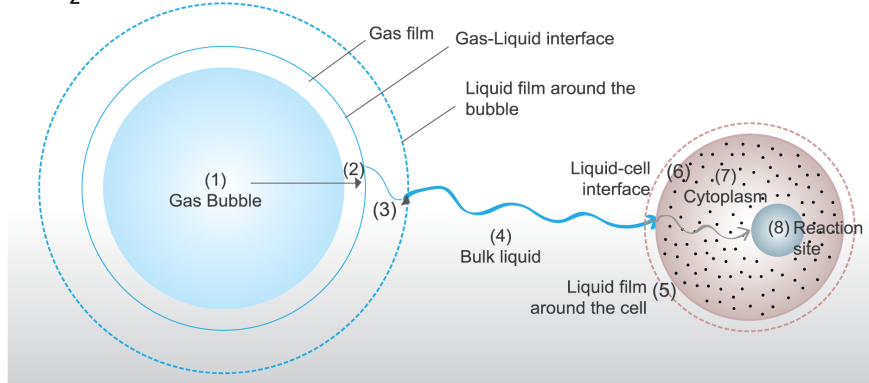
Figure 1. Analogy between the oxygen transfer model and the diffusion/reaction model. (A) Oxygen transfer from the gas bubble into the cell’s cytoplasm and subsequent reaction: (1) Transfer from the interior of the bubble to the gas–liquid interface; (2) Movement across the gas–liquid interface; (3) Diffusion through the relatively stagnant liquid film surrounding the bubble; (4) Transport through the bulk liquid; (5) Diffusion through the relatively stagnant liquid film surrounding the cells; (6) Movement across the liquid–cell interface; (7) Transport through the cytoplasm to the site where the reactions take place; (8) Biochemical reactions involving oxygen consumption. Adapted from Blanch and Clark¹⁰; (B) MP transport model in FISH: (1) MP diffusion through the medium to the cell membrane; (2) Membrane uptake of MP; (3) Cytoplasm diffusion within the cells to the nucleus; (4) Reaction between the MP and the target RNA.

Figure 2. Schematic representation of the MP’s diffusion in the bulk. l is the mean distance between the cell-centres, where the maximum distance for a MP to encounter a cell is $l/2$. This distance was further corrected by removing the diameter of each cell-type, considering the cell in the centre of the cube, in a vertical or horizontal orientation (for non-spherical cells). Considering a three-dimensional movement of the MPs, the mean square displacement ($\langle r(n)^2 \rangle$) is the hypotenuse of the Pythagoras’s theorem for the given geometric volume ($r(n)^2 = ((l/2)^2 + h^2)$).

Figure 3. Variation of the diffusional characteristic time (s) of a 10bp MP with the cellular size of most bacterial and animal cells (in radius, μm) and bulk cellular concentrations (cells/mL).

Figure 4 . Cellular membrane differences between bacterial cells and animal cells. The schematic representation is at scale considering the cell sizes displayed in Table 1. The bacterial cells are represented 5x times magnified.

A) O_2 transport model



B) Molecular Probes transport model

